Research Article
Implementation of an Approximate Conformal UPML in 2-D DGTD

Linqian Li,[1,2] Bing Wei,[1,2] Qian Yang,[1,2] and Debiao Ge[1,2]

[1]*School of Physics and Optoelectronic Engineering, Xidian University, Xi'an 710071, China*
[2]*Collaborative Innovation Center of Information Sensing and Understanding, Xidian University, Xi'an 710071, China*

Correspondence should be addressed to Linqian Li; llq11123@163.com

Using the numerical discrete technique with unstructured grids, conformal perfectly matched layer (PML) absorbing boundary in the discontinuous Galerkin time-domain (DGTD) can be set flexibly so as to save lots of computing resources. Based on the DGTD equations in an orthogonal curvilinear coordinate system, the processes of parameter transformation for 2-D UPML between the coordinate systems of elliptical and Cartesian are given; and the expressions of transition matrix are derived. The calculation scheme of conductivity distribution in elliptic cylinder absorbing layer is given, and the calculation coefficient of DGTD in elliptic UPML is calculated. Furthermore, the 2-D iterative formulas of DGTD and that of auxiliary equation in the elliptical cylinder UPML are derived; the conformal UPML calculation in DGTD is realized. Numerical results show that very good accuracy and computational efficiency are achieved by using the method in this paper. Compared to the rectangular computational region, both the memory and computation time of conformal UPML absorbing boundary are reduced by more than 20%.

1. Introduction

Truncated boundary condition is the key to ensure the accuracy for many electromagnetic numerical methods. In the past decades, different kinds of absorbing boundary conditions (ABC) have been proposed and successfully applied to the finite difference time-domain (FDTD) method and other methods. The perfectly matched layer (PML) ABC is presented by Berenger in 1994 [1]. Later, the coordinate stretched perfectly matched layer (CPML) ABC was proposed by Chew and Weedon [2], and uniaxial anisotropic perfectly matched layer (UPML) ABC was presented by Sacks et al. [3]. The conformal PML was analytically derived and applied to the hyperbolic model by Teixeira et al. in the 1990s [4–6]. The corner-free truncation strategy was proposed and used in FDTD method by Zhang et al. [7]. The discontinuous Galerkin time-domain (DGTD) [8–12] method, which was developed based on the finite volume element

time-domain method, has advantages of mesh flexibility of finite element time-domain (FETD) and explicit iterative of FDTD. As a new kind of time-domain algorithm, the study of ABC for DGTD is a hot topic in the computational electromagnetic field.

The first-order Silver-Muller (SM) ABC is widely used owing to its easy realization [13]. However, this kind of ABC only has a better absorption when the wave is perpendicular to the boundary. In order to avoid reflection, it is necessary to increase the distance between the scattering target and the absorption boundary; thus, the calculation amount is increased. Lu et al. introduced nonconforming UPML theory into DG calculations in the case of TM wave and compared the local relative error between PML and first-order SM-ABC [14]. König et al. applied the stretched-coordinate PML technique to DGTD [15]. Gedney and Zhao proposed a kind of auxiliary differential equation (ADE) multilevel PML theory by complex frequency domain shift, which is

used to cut off the boundary of DGTD region and take good absorption [16]. In the literature [17], the PML theory is used in 3-D DGTD algorithm to realize the absorption of electromagnetic wave through the conformal truncation face by Dosopoulos and Lee. Donderici and Teixeira incorporated conformal PML into the mixed FETD algorithm by utilizing PML constitutive tensors in 2008 [18]. Based on a higher-order curvilinear finite-element and the concept of transformation electromagnetics, Smull et al. proposed anisotropic locally conformal PML; this new PML has favorable accuracy and efficiency [19]. Modave et al. designed PMLs for transient acoustic wave propagation in generally shaped convex truncated domains in DGTD [20]. Yang et al. applied the corner-free truncation strategy to DGTD calculation, which saved the resource effectively [21]. Based on well-posed PML theory, Ren et al. proposed multiaxial full anisotropic media PML for subdomain and applied it to electromagnetic simulation of nonconformal mesh bicrystals; this method avoids the potential late-time instability found in classical PML [22]. However, many physical problems can be solved successfully by two-dimensional models. In two-dimensional models, it has advantages of small memory, fast calculation speed, easy handling the electromagnetic problem of electric large size by computer, and so on in three-dimensional models. Nevertheless, there is only little research focus on the study of DGTD method in two-dimensional problems. Implementation and application of conformal UPML in 2-D are not yet reported. In this paper, the 2-D DGTD iterative formula for elliptic cylindrical UPML is derived and applied to the nested dielectric column scattering.

In order to apply the UPML technique to DGTD in two-dimensional cases, the wave equations of UPML in an orthogonal curvilinear coordinate system are considered with the theory of parameter transformation, the processes of parameters transformation for 2-D UPML, and the specific expressions of transition matrix between the coordinate systems of elliptical and Cartesian are derived. The penalty flux is used for field exchange between units. The 2-D DGTD iterative formula and auxiliary equation in elliptical cylindrical UPML are derived. Numerical results show that very good effectiveness is achieved by using the proposed algorithm.

2. The Expression of UPML Equations from Orthogonal Curvilinear Coordinate System to Cartesian Coordinate System

Suppose that the interface from free space to PML is the isosurface ξ_3 in the orthogonal curve coordinate system (as shown in Figure 1); if the parameters in UPML satisfy the similar condition in Cartesian coordinate system UPML, the incident electromagnetic waves from free space will pass through the interface without reflecting and attenuate rapidly inside the PML.

2.1. UPML Wave Equation in Orthogonal Curvilinear Coordinate System. From the literature [17, 23], we know that the form of diagonal matrix of the parameters in the
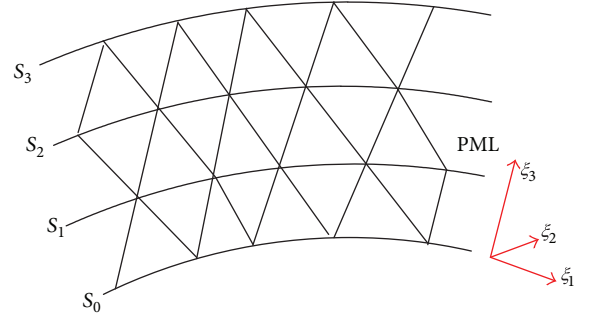

FIGURE 1: Discrete unit of PML in orthogonal curvilinear coordinate system.

orthogonal curve coordinate system is unchanged. So UPML matching matrix is written as follows:

$$
\begin{aligned}
\mathbf{\Lambda}_{u_1 u_2 u_3} &= \operatorname{diag}\left[\begin{array}{ccc} \dfrac{s_2 s_3}{s_1} & \dfrac{s_3 s_1}{s_2} & \dfrac{s_1 s_2}{s_3} \end{array}\right] \\
&= \mathbf{u}_1 \mathbf{u}_1 \dfrac{s_2 s_3}{s_1} + \mathbf{u}_2 \mathbf{u}_2 \dfrac{s_3 s_1}{s_2} + \mathbf{u}_3 \mathbf{u}_3 \dfrac{s_1 s_2}{s_3},
\end{aligned}
\tag{1}
$$

where $\mathbf{u}_1, \mathbf{u}_2, \mathbf{u}_3$ are unit vectors. And there are

$$
\begin{aligned}
s_1 &= \kappa_1 + \frac{\sigma_1}{j\omega\varepsilon_0}, \\
s_2 &= \kappa_2 + \frac{\sigma_2}{j\omega\varepsilon_0}, \\
s_3 &= \kappa_3 + \frac{\sigma_3}{j\omega\varepsilon_0}.
\end{aligned}
\tag{2}
$$

When the interface is the isosurface ξ_3 (as shown in Figure 1), the no-reflect condition is $s_1 = s_2 = 1$, then (1) is rewritten as follows:

$$
\mathbf{\Lambda}_{u_1 u_2 u_3} = \operatorname{diag}\left[\begin{array}{ccc} s_3 & s_3 & \dfrac{1}{s_3} \end{array}\right] = \mathbf{u}_1 \mathbf{u}_1 s_3 + \mathbf{u}_2 \mathbf{u}_2 s_3 + \mathbf{u}_3 \mathbf{u}_3 \dfrac{1}{s_3}.
\tag{3}
$$

UPML equations in an orthogonal curvilinear coordinate system are as follows:

$$
\begin{aligned}
\mu_1 \mathbf{a} \cdot \frac{\partial H}{\partial t} + \mu_1 \mathbf{b} \cdot H + \mu_1 \mathbf{c} \cdot P_h + \nabla \times E &= 0, \\
\varepsilon_1 \mathbf{a} \cdot \frac{\partial E}{\partial t} + \varepsilon_1 \mathbf{b} \cdot E + \varepsilon_1 \mathbf{c} \cdot P_e - \nabla \times H &= 0,
\end{aligned}
\tag{4}
$$

where E and H are electromagnetic fields; μ_1 and ε_1 are permittivity and permeability, respectively. $\mathbf{a}$, $\mathbf{b}$, and $\mathbf{c}$ are diagonal tensors. P_h and P_e are auxiliary variables, which are satisfied with the following relationship:

$$
\begin{aligned}
\frac{\partial P_h}{\partial t} + \mathbf{d} \cdot P_h - \boldsymbol{\kappa}^{-1} \cdot H &= 0, \\
\frac{\partial P_e}{\partial t} + \mathbf{d} \cdot P_e - \boldsymbol{\kappa}^{-1} \cdot E &= 0,
\end{aligned}
\tag{5}
$$

where $\mathbf{d}$ and $\boldsymbol{\kappa}^{-1}$ are the same as $\mathbf{a}$, $\mathbf{b}$, and $\mathbf{c}$. Their expressions are as follows:

$$\mathbf{a} = \mathrm{diag}\left[\frac{\kappa_2 \kappa_3}{\kappa_1} \quad \frac{\kappa_3 \kappa_1}{\kappa_2} \quad \frac{\kappa_1 \kappa_2}{\kappa_3} \right],$$

$$\mathbf{b} = \mathrm{diag}\left[\frac{1}{\kappa_1 \varepsilon_0}(\sigma_2 \kappa_3 + \sigma_3 \kappa_2 - a_{11}\sigma_1) \quad \frac{1}{\kappa_2 \varepsilon_0}(\sigma_3 \kappa_1 + \sigma_1 \kappa_3 - a_{22}\sigma_2) \quad \frac{1}{\kappa_3 \varepsilon_0}(\sigma_1 \kappa_2 + \sigma_2 \kappa_1 - a_{33}\sigma_3) \right],$$

$$\mathbf{c} = \mathrm{diag}\left[\frac{\sigma_2 \sigma_3}{\varepsilon_0^2} - b_{11}\frac{\sigma_1}{\varepsilon_0} \quad \frac{\sigma_3 \sigma_1}{\varepsilon_0^2} - b_{22}\frac{\sigma_2}{\varepsilon_0} \quad \frac{\sigma_1 \sigma_2}{\varepsilon_0^2} - b_{33}\frac{\sigma_3}{\varepsilon_0} \right], \quad (6)$$

$$\mathbf{d} = \mathrm{diag}\left[\frac{\sigma_1}{\kappa_1 \varepsilon_0} \quad \frac{\sigma_2}{\kappa_2 \varepsilon_0} \quad \frac{\sigma_3}{\kappa_3 \varepsilon_0} \right],$$

$$\boldsymbol{\kappa}^{-1} = \mathrm{diag}\left[\frac{1}{\kappa_1} \quad \frac{1}{\kappa_2} \quad \frac{1}{\kappa_3} \right].$$

In practical applications, (4) and (5) often need to be solved in Cartesian coordinates, thus, they are transformed from a curvilinear coordinate system by transformation matrix, which can be written as follows:

$$\mathbf{T} = \begin{bmatrix} u_{1x} & u_{1y} & u_{1z} \\ u_{2x} & u_{2y} & u_{2z} \\ u_{3x} & u_{3y} & u_{3z} \end{bmatrix}, \quad (7)$$

where $u_{1x}, u_{2x}, u_{3x}, \ldots$ are components of unit vectors $\mathbf{u}_1$, $\mathbf{u}_2$, and $\mathbf{u}_3$ in x, y, and z direction, respectively. Transformation matrix has a unitary nature [24].

Taking the example of tensor $\mathbf{a}$, the relationship of $\mathbf{a}$ from a curvilinear coordinate system to Cartesian coordinates is as follows:

$$\mathbf{a}_{xyz} = \mathbf{T}^{-1} \cdot \mathbf{a} \cdot \mathbf{T}. \quad (8)$$

It is noted that after the transformation, the $\mathbf{a}_{xyz}$ is not the diagonal matrix anymore.

2.2. The Parameter Calculation for Elliptic Cylinder UPML. Since the expression of the transformation matrix depends on the specific coordinate system, the process of calculational parameters in the elliptical cylinder UPML can be described as follows.

Let the ellipse cylindrical axis be z-axis, and the elliptic equation is as follows:

$$\frac{x^2}{a^2} + \frac{y^2}{b^2} = 1, \quad (9)$$

where a and b are the semimajor axis and semiminor axis, respectively. The variables w and t are introduced, and let

$$x = a \cos t,$$
$$y = b \sin t, \quad (10)$$

$$a = c \cosh w,$$
$$b = c \sinh w, \quad (11)$$
$$a^2 - b^2 = c^2\left(\cosh^2 w - \sinh^2 w\right) = c^2,$$

where $w \geq 0$, $0 \leq t \leq 2\pi$, and c is the focal distance. Its trail is shown in Figure 2. w represents the distance sum between focal points in the ellipse. The transformation matrix between local coordinate of elliptical system and Cartesian coordinate system is decided by rotating angle β (as shown in Figure 2), which is defined as included angle between normal vector $\widehat{w}$ and the x-axis in the Cartesian coordinate system.

From [25], we know that the tangent line equation of the observation point $P(x_P, y_P)$ on the ellipse is as follows:

$$y = -\frac{b^2}{y_P}\frac{x_P}{a^2}x + \frac{b^2}{y_P}. \quad (12)$$

The slope of the tangent line k is as follows:

$$k = \tan \alpha = -\frac{b^2 x_P}{a^2 y_P}, \quad (13)$$

where α is the included angle between tangent line and normal vector $\widehat{w}$. Then, the direction cosine and direction sine between tangential unit vectors and normal vector $\widehat{w}$ are as follows:

$$\cos \alpha = \frac{\pm 1}{\sqrt{1 + \tan^2 \alpha}},$$
$$\sin \alpha = \frac{\pm \tan \alpha}{\sqrt{1 + \tan^2 \alpha}}. \quad (14)$$

The β is as follows:

$$\tan \beta = \tan\left(\alpha - \frac{\pi}{2}\right) = \frac{a^2 y_P}{b^2 x_P}. \quad (15)$$

Then, the direction cosine and direction sine between normal unit vectors and x- and y-axes are as follows:

$$\cos \beta = \frac{\pm 1}{\sqrt{1 + \tan^2 \beta}},$$
$$\sin \beta = \frac{\pm \tan \beta}{\sqrt{1 + \tan^2 \beta}}. \quad (16)$$
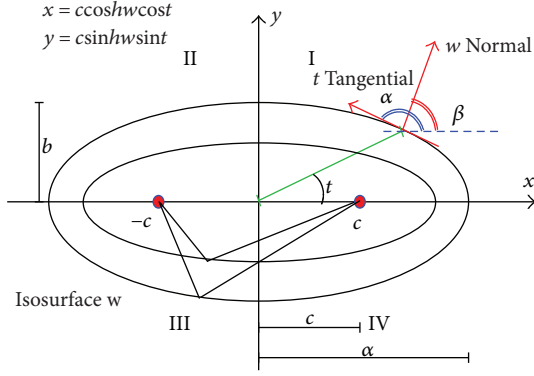
FIGURE 2: Elliptical cylinder coordinate systems.

Thus, the transformation matrix in (7) can be written as follows:

$$\mathbf{T}_{\text{oval}} = \begin{bmatrix} -\sin\beta & \cos\beta & 0 \\ 0 & 0 & 1 \\ \cos\beta & \sin\beta & 0 \end{bmatrix}. \tag{17}$$

Substituting (17) into (8), then

$$\mathbf{a}_{xyz} = \begin{bmatrix} a_{11}\sin^2\beta + a_{33}\cos^{02}\beta & (a_{33}-a_{11})\sin\beta\cos\beta & 0 \\ (a_{33}-a_{11})\sin\beta\cos\beta & a_{11}\cos^2\beta + a_{33}\sin^2\beta & 0 \\ 0 & 0 & a_{22} \end{bmatrix}$$

$$= \begin{bmatrix} a_{xx} & a_{xy} & 0 \\ a_{yx} & a_{yy} & 0 \\ 0 & 0 & a_{zz} \end{bmatrix}. \tag{18}$$

UPML are distributed between the regions $w_0 \le w \le w_{\text{max}}$. $\xi_3 = w$ in elliptical cylinder coordinate systems; thus, (2) is rewritten as follows:

$$\begin{aligned} s_1 &= s_\varphi = 1, \\ s_2 &= s_z = 1, \\ s_3 &= s_w = \kappa_w + \frac{\sigma}{j\omega\varepsilon_0}, \end{aligned} \tag{19}$$

where

$$\sigma = \sigma_{\text{max}} \left(\frac{w - w_0}{w_{\text{max}} - w_0} \right)^m, \tag{20}$$

where w is the isosurface of the ellipse in the barycentric coordinates of the element in UPML region. w_0 and w_{max} are the isosurface of the inside and the outside, respectively. m is taken as an integer.

Supposing that x_p, y_p, and focal distance c are known, we need to calculate the parameters of a, b_2 and w; the equation of the ellipse is

$$\frac{x_P^2}{a^2} + \frac{y_P^2}{b^2} = 1. \tag{21}$$

Thus, the formulas of semimajor axis a and semiminor axis b are

$$\begin{aligned} a^2 &= \left[\frac{-(x_P^2 - y_P^2 - c^2) \pm \sqrt{(x_P^2 - y_P^2 - c^2)^2 - 4c^2 x_P^2}}{2} \right], \\ b^2 &= a^2 - c^2, \end{aligned} \tag{22}$$

where $a^2 > c^2 > 0$.

Substituting (22) into (11), we can get

$$\cosh w = \frac{a}{c}, \quad w = \cosh^{-1}\left(\frac{a}{c}\right). \tag{23}$$

Inserting (23) into (20), we can obtain the value of conductivity σ.

3. Iterative Formulas of 2-D DGTD in Elliptical Cylinder UPML

In the case of two-dimensional TM wave, $E_x = E_y = 0$ and $H_z = 0$. Substituting (18) into (4), we can get

$$\begin{aligned} &\mu_1 \left(a_{xx} \frac{\partial H_x}{\partial t} + a_{xy} \frac{\partial H_y}{\partial t} \right) + \mu_1 \left(b_{xx} H_x + b_{xy} H_y \right) \\ &\quad + \mu_1 \left(c_{xx} P_{h,x} + c_{xy} P_{h,y} \right) + \frac{\partial E_z}{\partial y} = 0, \\ &\mu_1 \left(a_{yx} \frac{\partial H_x}{\partial t} + a_{yy} \frac{\partial H_y}{\partial t} \right) + \mu_1 \left(b_{yx} H_x + b_{yy} H_y \right) \\ &\quad + \mu_1 \left(c_{yx} P_{h,x} + c_{yy} P_{h,y} \right) - \frac{\partial E_z}{\partial x} = 0, \\ &\varepsilon_1 a_{zz} \frac{\partial E_z}{\partial t} + \varepsilon_1 b_{zz} E_z + \varepsilon_1 c_{zz} P_{e,z} - \left(\frac{\partial H_y}{\partial x} - \frac{\partial H_x}{\partial y} \right) = 0. \end{aligned} \tag{24}$$

The auxiliary equations in a two-dimensional case are

$$\begin{aligned} &\frac{\partial P_{h,x}}{\partial t} + d_{xx} P_{h,x} + d_{xy} P_{h,y} - \left(\kappa_{xx}^{-1} H_x + \kappa_{xy}^{-1} H_y \right) = 0, \\ &\frac{\partial P_{h,y}}{\partial t} + d_{yy} P_{h,y} + d_{yx} P_{h,x} - \left(\kappa_{yx}^{-1} H_x + \kappa_{yy}^{-1} H_y \right) = 0, \\ &\frac{\partial P_{e,z}}{\partial t} + d_{zz} P_{e,z} - \kappa_{zz}^{-1} E_z = 0 \Rightarrow \frac{\partial P_{e,z}}{\partial t} - E_z = 0. \end{aligned} \tag{25}$$

There are nondiagonal elements in (24) and (25), such as a_{xy}, a_{yx}, b_{xy}, b_{yx}, and so on. This will lead to a complex form of matrix equations. In order to facilitate the acquisition of the time-domain iterative formula, $\partial H_y/\partial t$ and $\partial H_x/\partial t$ in (24) need to be eliminated. Suppose that

$$A_1 = a_{xx}a_{yy} - a_{yx}a_{xy},$$
$$A_2 = a_{yy}b_{xx} - a_{xy}b_{yx},$$
$$A_3 = a_{yy}b_{xy} - a_{xy}b_{yy},$$
$$A_4 = a_{yy}c_{xx} - a_{xy}c_{yx},$$
$$A_5 = a_{yy}c_{xy} - a_{xy}c_{yy},$$
$$A_6 = a_{yy},$$
$$A_7 = a_{xy},$$
$$B_2 = a_{xx}b_{yy} - a_{yx}b_{xy}, \qquad (26)$$
$$B_3 = a_{xx}b_{yx} - a_{yx}b_{xx},$$
$$B_4 = a_{xx}c_{yx} - a_{yx}c_{xx},$$
$$B_5 = a_{xx}c_{yy} - a_{yx}c_{xy},$$
$$B_6 = a_{xx}, B_7 = a_{yx},$$
$$C_1 = c_{zz},$$
$$D_1 = d_{xy},$$
$$D_2 = d_{yx}.$$

Thus

$$\mu_1 A_1 \frac{\partial H_x}{\partial t} + \mu_1 A_2 H_x + \mu_1 A_3 H_y + \mu_1 A_4 P_{h,x}$$
$$+ \mu_1 A_5 P_{h,y} + A_6 \frac{\partial E_z}{\partial y} + A_7 \frac{\partial E_z}{\partial x} = 0,$$
$$\mu_1 A_1 \frac{\partial H_y}{\partial t} + \mu_1 B_2 H_y + \mu_1 B_3 H_x + \mu_1 B_4 P_{h,x} \qquad (27)$$
$$+ \mu_1 B_5 P_{h,y} - B_6 \frac{\partial E_z}{\partial x} - B_7 \frac{\partial E_z}{\partial y} = 0.$$

After using the penalty flux [11] as well as expending it by basic functions in (27), we can get

$$\mu_1 A_1 [M^m] \frac{\partial H_x}{\partial t} + \mu_1 A_2 [M^m] H_x + \mu_1 A_3 [M^m] H_y$$
$$+ \mu_1 A_4 [M^m] P_{h,x} + \mu_1 A_5 [M^m] P_{h,y} + A_6 [S_y] E_z + A_7 [S_x] E_z$$
$$+ \left\{ A_6 n_y \kappa_e^m F_{e,z} + A_6 n_y \nu_h^m n_x F_{h,y} - A_6 n_y \nu_h^m n_y F_{h,x} \right.$$
$$\left. + A_7 n_x \kappa_e^m F_{e,z} + A_7 n_x \nu_h^m n_x F_{h,y} - A_7 n_x \nu_h^m n_y F_{h,x} \right\} = 0,$$
$$\mu_1 A_1 [M^m] \frac{\partial H_y}{\partial t} + \mu_1 B_2 [M^m] H_y + \mu_1 B_3 [M^m] H_x$$
$$+ \mu_1 B_4 [M^m] P_{h,x} + \mu_1 B_5 [M^m] P_{h,y} - B_6 [S_x] E_z - B_7 [S_y] E_z$$
$$- \left\{ B_6 n_x \kappa_e^m F_{e,z} + B_6 n_x \nu_h^m n_x F_{h,y} - B_6 n_x \nu_h^m n_y F_{h,x} \right.$$
$$\left. + B_7 n_y \kappa_e^m F_{e,z} + B_7 n_y \nu_h^m n_x F_{h,y} - B_7 n_y \nu_h^m n_y F_{h,x} \right\} = 0,$$
$$\varepsilon_1 a_{zz} [M^m] \frac{\partial E_z}{\partial t} + \varepsilon_1 b_{zz} [M^m] E_z + \varepsilon_1 C_1 [M^m] P_{e,z}$$
$$- [S_x] H_y + [S_y] H_x + \kappa_h^m \left(n_y F_{h,x} - n_x F_{h,y} \right) - \nu_e^m F_{e,z} = 0.$$
$$(28)$$

After (28) is discrete in time axis, then there are

$$H_{x,n+1/2} = \alpha_{hx} H_{x,n-1/2} - \beta_{hx} A_3 H_{y,n-1/2} - \beta_{hx} A_4 P_{h,x,n}$$
$$- \beta_{hx} A_5 P_{h,y,n} - \beta_{hx} \frac{1}{\mu_1} [M^m]^{-1}$$
$$\cdot \left\{ \left(A_6 [S_y] + A_7 [S_x] \right) E_{z,n} + A_6 \kappa_e^m n_y F_{e,z,n} \right.$$
$$+ A_6 \nu_h^m n_x n_y F_{h,y,n-1/2} - A_6 \nu_h^m n_y n_y F_{h,x,n-1/2}$$
$$+ A_7 \kappa_e^m n_x F_{e,z,n} + A_7 \nu_h^m n_x n_x F_{h,y,n-1/2}$$
$$\left. - A_7 \nu_h^m n_x n_y F_{h,x,n-1/2} \right\}.$$
$$H_{y,n+1/2} = \alpha_{hy} H_{y,n-1/2} - \beta_{hy} B_3 H_{x,n-1/2} - \beta_{hy} B_4 P_{h,x,n}$$
$$- \beta_{hy} B_5 P_{h,y,n} + \beta_{hy} \frac{1}{\mu_1} [M^m]^{-1}$$
$$\cdot \left\{ \left(B_6 [S_x] + B_7 [S_y] \right) E_{z,n} + B_6 \kappa_e^m n_x F_{e,z,n} \right.$$
$$+ B_6 \nu_h^m n_x n_x F_{h,y,n-1/2} - B_6 \nu_h^m n_x n_y F_{h,x,n-1/2}$$
$$+ B_7 \kappa_e^m n_y F_{e,z,n} + B_7 \nu_h^m n_y n_x F_{h,y,n-1/2}$$
$$\left. - B_7 \nu_h^m n_y n_y F_{h,x,n-1/2} \right\},$$
$$E_{z,n+1} = \alpha_{ez} E_{z,n} - C_1 \beta_{ez} P_{e,z,n+1/2} + \beta_{ez} \frac{1}{\varepsilon_1} [M^m]^{-1}$$
$$\cdot \left\{ [S_x] H_{y,n+1/2} - [S_y] H_{x,n+1/2} \right.$$
$$\left. - \kappa_h^m \left(n_y F_{h,x,n+1/2} - n_x F_{h,y,n+1/2} \right) + \nu_e^m F_{e,z,n} \right\}.$$
$$(29)$$

The iterative formulas of auxiliary equations are

$$P_{h,x,n+1} = c_h \cdot P_{h,x,n} - c_i \cdot D_1 P_{h,y,n} + c_i$$
$$\cdot \left(\kappa_{xx}^{-1} H_{x,n+1/2} + \kappa_{xy}^{-1} H_{y,n+1/2} \right),$$
$$P_{h,y,n+1} = c_j \cdot P_{h,y,n} - c_k \cdot D_2 P_{h,x,n} + c_k \qquad (30)$$
$$\cdot \left(\kappa_{yx}^{-1} H_{x,n+1/2} + \kappa_{yy}^{-1} H_{y,n+1/2} \right),$$
$$P_{e,z,n+1/2} = P_{e,z,n-1/2} + \Delta t E_{z,n},$$

where α_{hx}, β_{hx}, α_{hy}, β_{hy}, α_{ez}, β_{ez}, c_h, c_h, c_j, and c_k are iterative coefficients.

4. Numerical Examples

In the elliptical cylindrical computing region, the semimajor and semishort axes of the outer PML boundary are 4 m and 3 m, respectively. And the inner PML boundary has a semimajor axis of 3.5 m. Both the inner and outer PML boundaries have the same focus length of 2.29 m. The region is divided into 46,122 triangular units and 23,298 nodes with the discrete scale of 0.05 m. The time discrete interval is taken as dt = 0.16×10^{-10} s. The radiant source of Gaussian impulse which has the width and peak of $\tau = 200$ dt and $t_0 = 100$ dt is set at the center of the region (0 m, 0 m). Time-domain waveform and spectrum at the monitoring point of (0, 2.5 m) are shown in Figure 3(a). The solid and dotted line are the impulse waveform in time-domain and the spectrum,
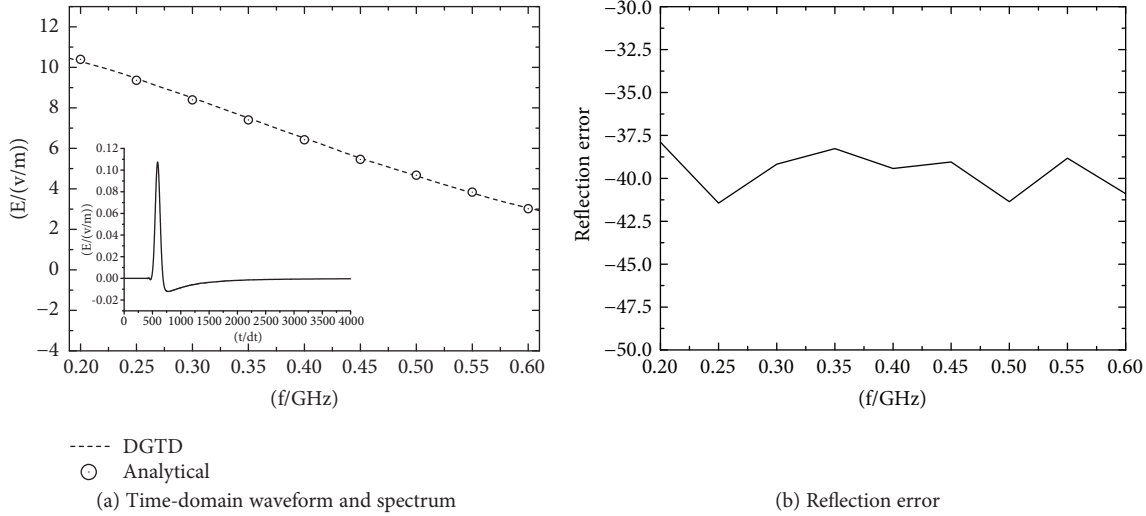
(a) Time-domain waveform and spectrum

----- DGTD
○ Analytical

(b) Reflection error

FIGURE 3: Radiant field and reflection error.

○ DGTD
— MoM

FIGURE 4: Bistatic RCS of PEC elliptic column.

(a) Sparse discrete model

○ DGTD conformal PML
▲ DGTD rectangular PML
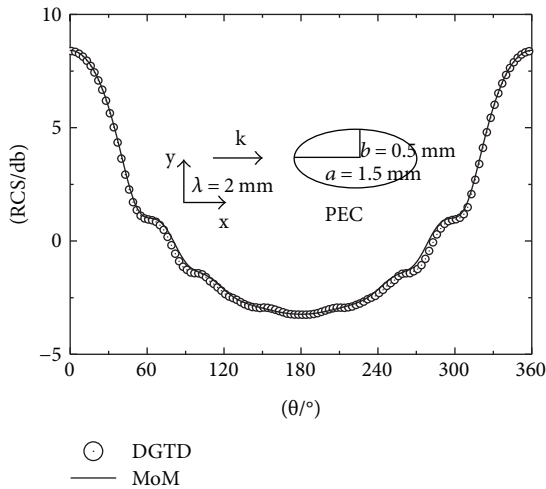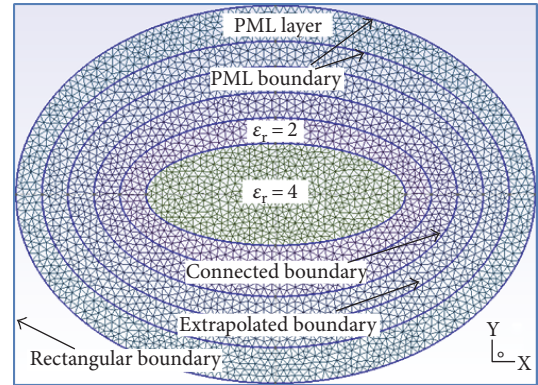— FDTD

(b) Bistatic RCS for two nested elliptical columns
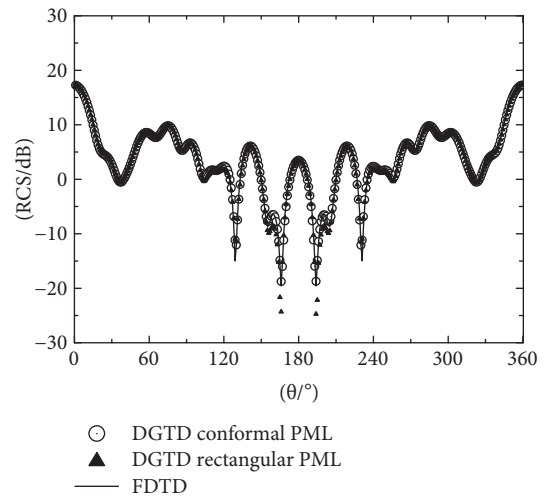
FIGURE 5: Bistatic scattering for target.

respectively. And "o" is the analytic solution obtained by the second kind of zero order Hankel function. Refer to [18]; the resulting reflection error is shown in Figure 3(b). It can be seen from the figure that the reflection error is below −37 dB.

The PEC elliptic column has a semimajor axis and a semishort axis of 1.5 mm and 0.5 mm, respectively. Incident plane wave has a wavelength of 2 mm. The computational region is truncated with conformal PML layer. The result of bistatic scattering for metal elliptical column is shown in Figure 4 ("o"). For easy comparison, the result of method of moment (solid line) is also shown in figure. As illustrated, the results are consistent.

Two nested dielectric elliptical columns target truncated by conformal PML. Sparse discrete conformal model is shown in Figure 5(a). The inner elliptical target has a relative dielectric coefficient of 4, and the semimajor axis and semiminor axis are 5 mm and 2 mm, respectively. The outer has a relative dielectric coefficient of 2, which are 6 mm and 3 mm. The rest of conformal boundaries from inside to

outside are connected boundary, extrapolated boundary, and PML boundary. Both the inner and outer PML boundaries have the same focus distance. The calculating region is

TABLE 1: Comparison of the number of unit and node in different calculated regions.

Shape	Discrete scale							
	0.1 mm		0.04 mm		0.08 mm			
	Number of unit	Number of node	Number of unit	Number of node	Number of unit	Number of node	Storages (MB)	Time (mins)
Nonconformal	77,670	39,184	489,534	245,638	121,474	61,175	116.5	134.7
Conformal	61,088	30,821	383,690	192,534	94,634	47,662	92.8	101.6

divided into 94,634 triangular units and 47,662 nodes with the discrete scale of 0.08 mm. The incident plane wave has a wavelength of 3 mm. Bistatic RCS for coated dielectric elliptical column target is shown in Figure 5(b) ("o"). The results of FDTD (solid line) and DGTD ("▲") (its region is truncated with rectangular PML) are also shows in the figure. As can be seen, the calculation results of the three coincide.

In order to verify the benefits of conformal UPML, the numbers of unit and node in two different regions by three discrete scales of 0.1 mm, 0.08 mm, and 0.04 mm are given in Table 1. Compared to the elliptical region, their numbers in rectangular computational region (the region surrounded by rectangular boundary which is shown in Figure 5(a)) increase by about 27%. In order to further compare the time and memory consumption, the following calculation is given. Take the case of discrete scale of 0.08 mm example (shown in Table 1), the numbers of unit and node in rectangular region are 121,474 and 61,175, respectively, which increase by 28.3%. And the memory and time increase by 25.5% and 32.5%, respectively. It is clear that conformal UPML has obvious advantages in terms of computational resources and computational time savings.

5. Conclusions

According to the DGTD equations and the parameter transformation theory in orthogonal curvilinear coordinate systems, the processes of parameter transformation for 2-D UPML between the coordinate systems of elliptical and Cartesian are presented, and expressions of transition matrix are derived. The 2-D iterative formulas of DGTD and that of auxiliary equation in elliptical cylinder UPML are derived, and the conformal UPML calculation in DGTD are realized. Numerical results show that good absorption for the outgoing wave can be realized by using conformal UPML. Because of the discrete characteristics of the unstructured grids, the absorption layer can be set up flexibly according to the shape of the target. Compared with the computational cost in rectangular PML layer, the memory and computation time for conformal structure decrease by 20.3% and 24.5%, respectively. Thus, the method presented in this paper will be very beneficial to the engineering computation since lots of computing resources can be saved.

Conflicts of Interest

The authors declare that there is no conflict of interests regarding the publication of this paper.

References

[1] J. P. Berenger, "A perfectly matched layer for the absorption of electromagnetic waves," *Journal of Computational Physics*, vol. 114, no. 2, pp. 185–200, 1994.

[2] W. C. Chew and W. H. Weedon, "A 3D perfectly matched medium from modified Maxwell's equations with stretched coordinates," *Microwave and Optical Technology Letters*, vol. 7, no. 13, pp. 599–604, 1994.

[3] Z. S. Sacks, D. M. Kingsland, R. Lee, and J.-F. Lee, "A perfectly matched anisotropic absorber for use as an absorbing boundary condition," *IEEE Transactions on Antennas and Propagation*, vol. 43, no. 12, pp. 1460–1463, 1995.

[4] F. L. Teixeira and W. C. Chew, "Analytical derivation of a conformal perfectly matched absorber for electromagnetic waves," *Microwave and Optical Technology Letters*, vol. 17, no. 4, pp. 231–236, 1998.

[5] K.-P. Hwang and J.-M. Jin, "Application of a hyperbolic grid generation technique to a conformal PML implementation," *IEEE Microwave and Guided Wave Letters*, vol. 9, no. 4, pp. 137–139, 1999.

[6] F. L. Teixeira, K.-P. Hwang, W. C. Chew, and J.-M. Jin, "Conformal PML-FDTD schemes for electromagnetic field simulations: a dynamic stability study," *IEEE Transactions on Antennas and Propagation*, vol. 49, no. 6, pp. 902–907, 2001.

[7] Y. Zhang, N. Feng, H. Zheng, and H. Liu, "A corner-free truncation strategy in three-dimensional FDTD computation," *IEEE Transactions on Electromagnetic Compatibility*, vol. 58, no. 2, pp. 512–522, 2016.

[8] I. Perugia and D. Schötzau, "The ^{hp}-local discontinuous Galerkin method for low-frequency time-harmonic Maxwell equations," *Mathematics of Computation*, vol. 72, no. 243, pp. 1179–1214, 2003.

[9] B. Cockburn, F. Li, and C. W. Shu, "Locally divergence-free discontinuous Galerkin methods for the Maxwell equations," *Journal of Computational Physics*, vol. 194, no. 2, pp. 588–610, 2004.

[10] J. Chen and Q. H. Liu, "Discontinuous Galerkin time-domain methods for multiscale electromagnetic simulations: a review," *Proceedings of the IEEE*, vol. 101, no. 2, pp. 242–254, 2013.

[11] J. Alvarez, *A Discontinuous Galerkin Finite Element Method for the Time-Domain Solution of Maxwell Equations*, University of Granada, Spain, 2013.

[12] S. Yan and J. M. Jin, "A dynamic *p*-adaptive DGTD algorithm for electromagnetic and multiphysics simulations," *IEEE*

Transactions on Antennas and Propagation, vol. 65, no. 5, pp. 2446–2459, 2017.

[13] P. Bonnet, X. Ferrieres, B. L. Michielsen, P. Klotz, and J. L. Roumiguières, "Finite-volume time domain method," in *Time Domain Electromagnetics*, pp. 307–368, Acade Press, San Diego, CA, USA, 1999.

[14] T. Lu, P. Zhang, and W. Cai, "Discontinuous Galerkin methods for dispersive and lossy Maxwell's equations and PML boundary conditions," *Journal of Computational Physics*, vol. 200, no. 2, pp. 549–580, 2004.

[15] M. König, C. Prohm, K. Busch, and J. Niegemann, "Stretched-coordinate PMLs for Maxwell's equations in the discontinuous Galerkin time-domain method," *Optics Express*, vol. 19, no. 5, pp. 4618–4631, 2011.

[16] S. D. Gedney and B. Zhao, "An auxiliary differential equation formulation for the complex-frequency shifted PML," *IEEE Transactions on Antennas and Propagation*, vol. 58, no. 3, pp. 838–847, 2010.

[17] S. Dosopoulos and J. F. Lee, "Interior penalty discontinuous Galerkin finite element method for the time-dependent first order Maxwell's equations," *IEEE Transactions on Antennas and Propagation*, vol. 58, no. 12, pp. 4085–4090, 2010.

[18] B. Donderici and F. L. Teixeira, "Conformal perfectly matched layer for the mixed finite element time-domain method," *IEEE Transactions on Antennas and Propagation*, vol. 56, no. 4, pp. 1017–1026, 2008.

[19] A. P. Smull, A. B. Manic, S. B. Manic, and B. M. Notaros, "Anisotropic locally-conformal perfectly matched layer for higher order curvilinear finite-element modeling," *IEEE Transactions on Antennas and Propagation*, vol. 65, no. 12, pp. 7157–7165, 2017.

[20] A. Modave, J. Lambrechts, and C. Geuzaine, "Perfectly matched layers for convex truncated domains with discontinuous Galerkin time domain simulations," *Computers & Mathematics with Applications*, vol. 73, no. 4, pp. 684–700, 2017.

[21] Q. Yang, B. Wei, L. Li, and D. Ge, "Implementation of corner-free truncation strategy in DGTD method," *Waves in Random and Complex Media*, vol. 27, no. 2, pp. 367–380, 2017.

[22] Q. Ren, Q. Zhan, and Q. H. Liu, "An improved subdomain level non-conformal discontinuous Galerkin time domain (DGTD) method for materials with full-tensor constitutive parameters," *IEEE Photonics Journal*, vol. 9, no. 2, article 2600113, 2017.

[23] F. L. Teixeira and W. C. Chew, "Systematic derivation of anisotropic PML absorbing media in cylindrical and spherical coordinates," *IEEE Microwave and Guided Wave Letters*, vol. 7, no. 11, pp. 371–373, 1997.

[24] D. B. Ge and B. Wei, *Electromagnetic Wave Theory*, Science Press, Beijing, 2011.

[25] L. X. Wang, D. Z. Fang, and M. Y. Zhang, *Mathematics Manual*, People's Education Press, Beijing, 1979.